Chiral discrimination upon crystallisation of the diastereomeric salts of 1-arylethylamines with mandelic acid or *p*-methoxymandelic acid: interpretation of the resolution efficiencies on the basis of the crystal structures

Kazushi Kinbara,[a] Kenichi Sakai,[b] Yukihiko Hashimoto,[a] Hiroyuki Nohira[b] and Kazuhiko Saigo*[,a]

[a] *Department of Chemistry and Biotechnology, Graduate School of Engineering, The University of Tokyo, Hongo, Bunkyo-ku, Tokyo 113, Japan*
[b] *Department of Applied Chemistry, Faculty of Engineering, Saitama University, Shimo-ohkubo, Urawa, Saitama 338, Japan*

The crystal structures of the diastereomeric salts of 1-arylethylamines with mandelic acid or *p*-methoxymandelic acid have been studied. This revealed that there was correlation between the efficiencies of the optical resolutions of the amines with the resolving reagents and the crystal structures of the salts. A characteristic hydrogen-bond layer, consisting of stable columnar structures and having a planar boundary surface, was found to be common to the less-soluble salt crystals; these crystals were considered to be stabilised from the viewpoint of both their hydrogen-bonding and van der Waals interactions. In contrast, in the corresponding more-soluble salts and in those diastereomeric salts which could not be separated by crystallisation, no such particularly stabilised crystal structure was formed; there only existed either columnar structures or planar boundary surfaces in these crystals. These results strongly suggest that for successful resolution it is necessary to realise a hydrogen-bond layer, consisting of stable columns and having planar boundary surfaces, in the crystals of one of the pair of diastereomeric salts. In order to achieve such a crystal structure, complementarity in molecular length between a target racemate and a resolving reagent must be considered the most important and fundamental factor.

Optical resolution *via* diastereomeric salt formation is the most convenient and commonly used method for separating enantiomers of a given racemic acid or base.[1] However, despite the practical importance of this method, the mechanism of chiral discrimination upon crystallisation is not yet sufficiently understood.

Recently, the crystal structures of some diastereomeric salts have been determined, and the role of the hydrogen-bond networks formed in these crystals in chiral discrimination has been studied for non-systematically selected compounds.[2] However, the correlations between the characteristics of the crystal structures of diastereomeric salts and the effectiveness of resolving reagents is not well understood at present; the study has not yet achieved its most important end, the rational design of resolving reagents.

In our previous paper, we reported that similarity in molecular length between a target racemate and a resolving reagent is the most important factor for achieving successful optical resolution; in the resolution of 1-arylethylamines with mandelic acid (**1**) or its derivatives, *p*-substituted mandelic acids were found to be suitable resolving reagents for *p*-substituted 1-arylethylamines, while **1** was found to be suitable for non- or *o*-substituted 1-arylethylamines.[3] These results strongly suggest that there would be a common mechanism for the chiral discrimination of 1-arylethylamines by mandelic acid or its derivatives. Since the solubility of a salt depends on its crystal structure to a considerable extent, a crystallographic study of the crystal structures of a pair of the diastereomeric salts should help clarify the mechanism of chiral discrimination.

In the present paper we describe details of the crystal structures of several pairs of diastereomeric salts of 1-arylethylamines with **1** or *p*-methoxymandelic acid **2**, and rationalise our previous proposal concerning the choice of a suitable resolving reagent on the basis of these crystallographic analyses.

Results and discussion

Crystal structures of less-soluble (*R*)-1·(*R*)-3, (*R*)-1·(*S*)-4 and (*R*)-1·(*R*)-5

Our previous results on the optical resolution of 1-arylethylamines **3**–**8** with (*R*)-**1** or (*R*)-**2** are summarised in

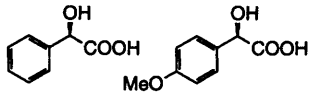

1 **2**

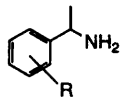

3: R=H
4: R=*o*-Me
5: R=*m*-OMe
6: R=*m*-Me
7: R=*p*-OMe
8: R=*p*-Me

Table 1.[3] Amines **3**–**5**, having a similar molecular length to that of (*R*)-**1**, could be efficiently resolved by (*R*)-**1**. In contrast, amines **6**–**8**, having a greater molecular length than that of (*R*)-**1**, could not be resolved by (*R*)-**1**, while (*R*)-**2** was suitable for these amines.

In order to explain these results, we first studied the crystal structures of the less-soluble salts of **3**–**5** with (*R*)-**1** [(*R*)-**1**·(*R*)-**3**,[4] (*R*)-**1**·(*S*)-**4** and (*R*)-**1**·(*R*)-**5**[5]], all of which were efficiently resolved by (*R*)-**1** (Table 1, entries 1–3).

As a result, it was found that in the crystals of these less-soluble salts, a common, quite characteristic hydrogen-bond network was formed. Two pairs of mandelate anions and the primary ammonium cations form a unit, in which the pairs are related to each other by a twofold screw axis, constructed

Table 1 Resolution of 1-arylethylamines **3–8** with (*R*)-**1** or (*R*)-**2**

Entry	Racemic amine	Resolving reagent	Solvent	Yield (%)[a]	Ee (%)[b]	Resolution efficiency[c]
1	**3**	**1**	H_2O	76	87[d]	0.66
2	**4**	**1**	H_2O	71	100[e]	0.71
3	**5**	**1**	MeOH	70	89[d]	0.62
4	**6**	**1**	MeOH	94	12[f]	0.11
5	**7**	**1**	MeOH	84	4[f]	0.03
6	**8**	**1**	MeOH	88	4[e]	0.04
7	**3**	**2**	MeOH	70	89[d]	0.62
8	**6**	**2**	MeOH	76	75[f]	0.57
9	**7**	**2**	MeOH	62	46[f]	0.29
10	**8**	**2**	MeOH	72	85[d]	0.61

[a] Yield of the crystallised diastereomeric salt based on half the amount of the racemic amine. [b] Enantiomeric excess (ee) of the liberated amine after a single crystallisation of the diastereomeric salt. [c] Defined as the product of the yield of the diastereomeric salt and the ee of the liberated amine. [d] (*R*)-Amine was obtained as the major enantiomer. [e] (*S*)-Amine was obtained as the major enantiomer. [f] The absolute configuration of the major isomer was not determined.

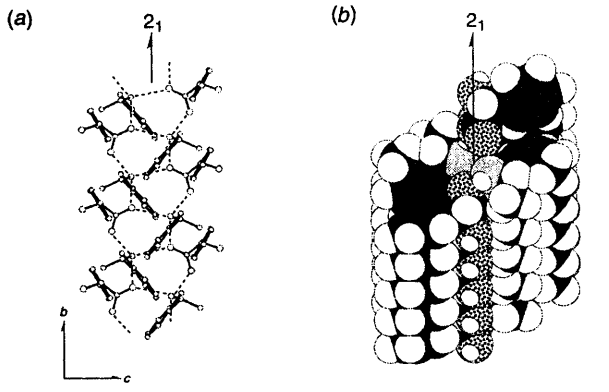

Fig. 1 Typical columnar hydrogen bonds in the crystal of a less-soluble diastereomeric salt, exemplified by less-soluble (*R*)-**1**·(*S*)-**4**: (*a*) ORTEP drawing viewed down the *a* axis. The dashed lines show the hydrogen bonds. (*b*) Space-filling model of the hydrogen-bond column.

through three kinds of hydrogen bonds between the carboxylate oxygens and the three ammonium hydrogens. Each unit has hydrogen bonds with translational neighbouring units, resulting in the formation of an infinite columnar structure (Fig. 1).[6] Such an infinite columnar structure (2_1-column) is frequently found in the crystal structures of the salts of primary amines with carboxylic acids.[7] These facts suggest that the most common and stable crystal packing for the salts of ammonium cations with carboxylate anions is realised in the crystals of less-soluble (*R*)-**1**·(*R*)-**3**, (*R*)-**1**·(*S*)-**4** and (*R*)-**1**·(*R*)-**5**. Neighbouring 2_1-columns are interlinked by an intermolecular –OH···O hydrogen bond between the hydroxy hydrogen of a (*R*)-**1** molecule and the carboxylate oxygen of another (*R*)-**1** molecule, providing an infinite hydrogen-bond layer [Figs. 2(*a*)–4(*a*) for (*R*)-**1**·(*R*)-**3**, (*R*)-**1**·(*S*)-**4** and (*R*)-**1**·(*R*)-**5**, respectively], which is rather stable and favourable from the viewpoint of hydrogen-bonding interactions.

This hydrogen-bond layer has a further characteristic, its boundary surfaces are planar [Figs. 2(*b*)–4(*b*)]. As a result, quite close packing of the layers is realised in forming a three-dimensional crystal; the layers would be efficiently stabilised by van der Waals interactions between them.

Thus, all of the crystals of less-soluble (*R*)-**1**·(*R*)-**3**, (*R*)-**1**·(*S*)-**4** and (*R*)-**1**·(*R*)-**5** are considered to be stabilised from the viewpoint of both their hydrogen-bonding and van der Waals interactions.

Crystal structures of more-soluble (*S*)-**1**·(*R*)-**3** and (*S*)-**1**·(*R*)-**5**

In the next stage, we focused our attention on the crystal structures of the more-soluble diastereomeric salts of **1**, and compared their crystal structures with those of the corresponding less-soluble salts.

In the crystal of more-soluble (*S*)-**1**·(*R*)-**3** [the same molecular arrangement as (*R*)-**1**·(*S*)-**3** but in mirror image (Fig. 5)],[8] a quite complicated hydrogen-bond network, whose pattern was largely different from that of the corresponding less-soluble salt [(*R*)-**1**·(*R*)-**3**], was found; stable 2_1-columns, constructed by carboxylate and ammonium groups, were not formed, while four pairs of crystallographically nonequivalent mandelates and ammoniums form an infinite hydrogen-bond layer through sixteen kinds of hydrogen bonds. Furthermore, in this hydrogen-bond network, two of the hydrogen-acceptors are hydroxy oxygens, which are less favourable than carboxylate oxygens. This fact is not in accordance with the rule of hydrogen bonding proposed by Etter that the best hydrogen donor will form a hydrogen bond with the best hydrogen acceptor.[9] Therefore, we consider this hydrogen-bond layer to be less stable than that of the less-soluble (*R*)-**1**·(*R*)-**3** from the viewpoint of hydrogen-bonding interactions. On the other hand, the boundary surfaces of the layer are almost planar, and close packing of the layers is achieved [Fig. 5(*b*)], which is favourable from the viewpoint of van der Waals interactions between the layers.

In the crystal of more-soluble (*S*)-**1**·(*R*)-**5**, an infinite hydrogen-bond layer comprising 2_1-columns was found, like those of less-soluble (*R*)-**1**·(*R*)-**3**, (*R*)-**1**·(*S*)-**4** and (*R*)-**1**·(*R*)-**5** [Fig. 6(*a*)]; this crystal is considered to be stable from the viewpoint of its hydrogen-bonding interactions. However, the methoxy group on the phenyl group of **5** projects out of the layer, making its boundary surfaces uneven. This deformation should result in a looser packing of the layers, compared to that of less soluble (*R*)-**1**·(*R*)-**5** [Fig. 6(*b*)];[10] therefore packing of the layers is not efficiently stabilised by van der Waals interactions.

These comparisons of the crystal structures of two pairs of less- and more-soluble diastereomeric salts indicate that the less-soluble salt is efficiently stabilised by two interactions, *i.e.* hydrogen-bonding and van der Waals interactions, whereas the more-soluble salts are stabilised by only one of these. Namely, the less-soluble salts are much more stable than the corresponding more-soluble salts, resulting in the preferential precipitation of one of the diastereomeric salts upon crystallisation.

Crystal structures of the salts of **8** with **1**

Subsequently, we studied the crystal structures of the individual diastereomeric salts of **8** with (*R*)-**1** [(*R*)-**1**·(*R*)-**8** and (*R*)-**1**·(*S*)-**8**], which could not be separated by recrystallisation (Table 1, entry 6).

In the crystal of (*R*)-**1**·(*R*)-**8**, a quite complicated pattern of hydrogen-bonds was observed (Fig. 7). Four pairs of crystallographically nonequivalent mandelates and ammoniums form an infinite hydrogen-bond layer through sixteen kinds of hydrogen bonds, in which two of the hydrogen acceptors are hydroxy oxygens; this crystal structure is quite similar to that of (*S*)-**1**·(*R*)-**3**. Since stable 2_1-columns, which are common to the

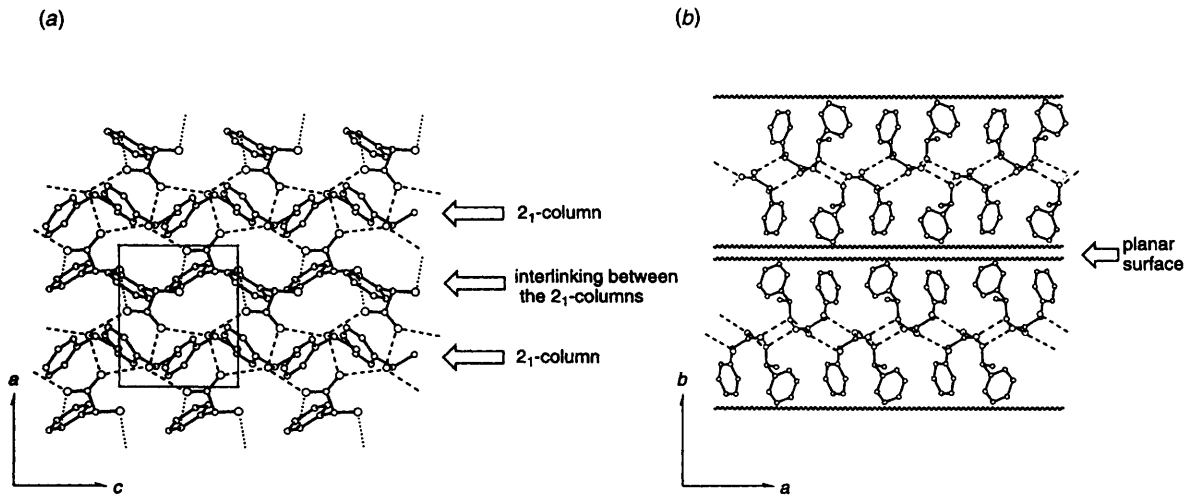

Fig. 2 Crystal structure of less-soluble (*R*)-**1**·(*R*)-**3**.[4] (*a*) Viewed down the *b* axis. The dashed lines indicate the hydrogen bonds, which form the columns. The dotted lines indicate the hydrogen bonds, which interlink the columns. The solid lines show the unit cell. (*b*) Viewed down the *c* axis. The dashed lines show the hydrogen bonds. The wavy lines show the boundary surfaces of the layer.

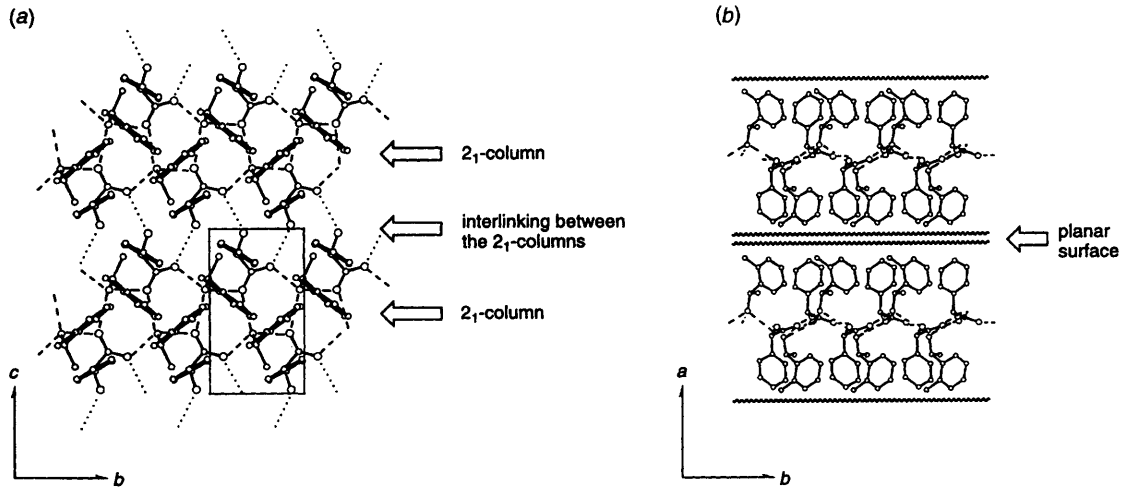

Fig. 3 Crystal structure of less-soluble (*R*)-**1**·(*S*)-**4**. (*a*) Viewed down the *a* axis. The dashed lines indicate the hydrogen bonds, which form the columns. The dotted lines indicate the hydrogen bonds, which interlink the columns. The solid lines show the unit cell. (*b*) Viewed down the *c* axis. The dashed lines show hydrogen bonds. The wavy lines show the boundary surfaces of the layer.

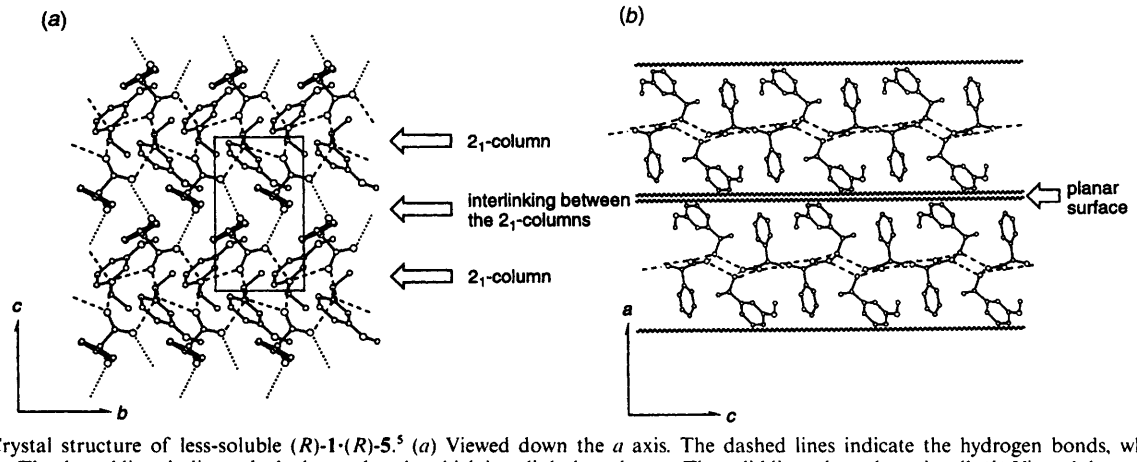

Fig. 4 Crystal structure of less-soluble (*R*)-**1**·(*R*)-**5**.[5] (*a*) Viewed down the *a* axis. The dashed lines indicate the hydrogen bonds, which form the colums. The dotted lines indicate the hydrogen bonds, which interlink the columns. The solid lines show the unit cell. (*b*) Viewed down the *b* axis. The dashed lines show the hydrogen bonds. The wavy lines show the boundary surfaces of the layer.

less-soluble salts [(*R*)-**1**·(*R*)-**3**, (*R*)-**1**·(*S*)-**4** and (*R*)-**1**·(*R*)-**5**], are not formed in this case, this crystal structure seems to be less stable than those of the less-soluble salts from the viewpoint of its hydrogen-bonding interactions, just as in the case of the more-soluble (*S*)-**1**·(*R*)-**3**. However, the boundary surfaces of the layer are almost planar, and hence close packing of the layers is achieved [Fig. 7(*b*)].

On the other hand, the crystal structure of (*R*)-**1**·(*S*)-**8** is

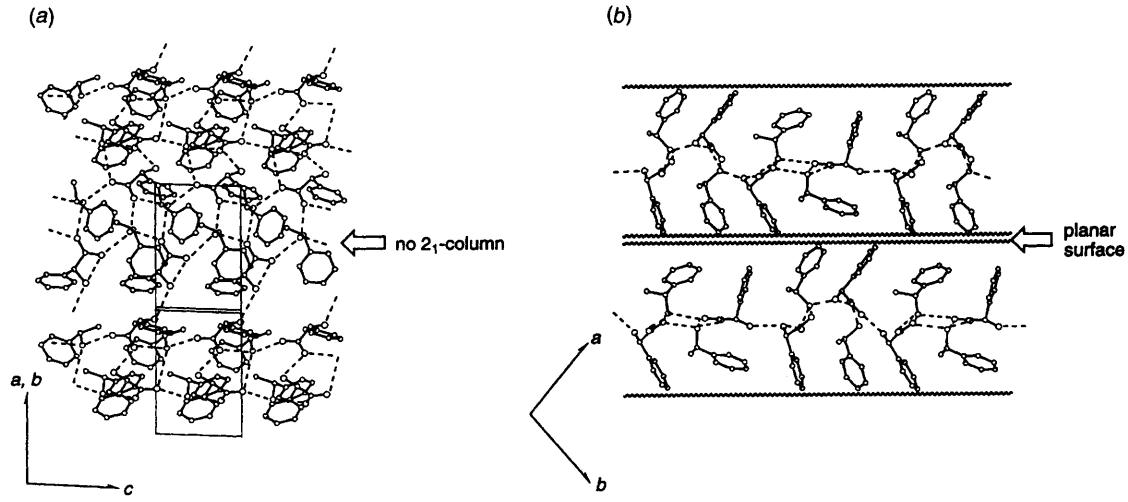

Fig. 5 Crystal structure of more-soluble (*S*)-**1**·(*R*)-**3**.[8] (*a*) Viewed perpendicular to the hydrogen-bond layer. The solid and dashed lines show the unit cell and hydrogen bonds, respectively. (*b*) Viewed parallel to the layer. The dashed lines show the hydrogen bonds. The wavy lines show the boundary surfaces of the layer.

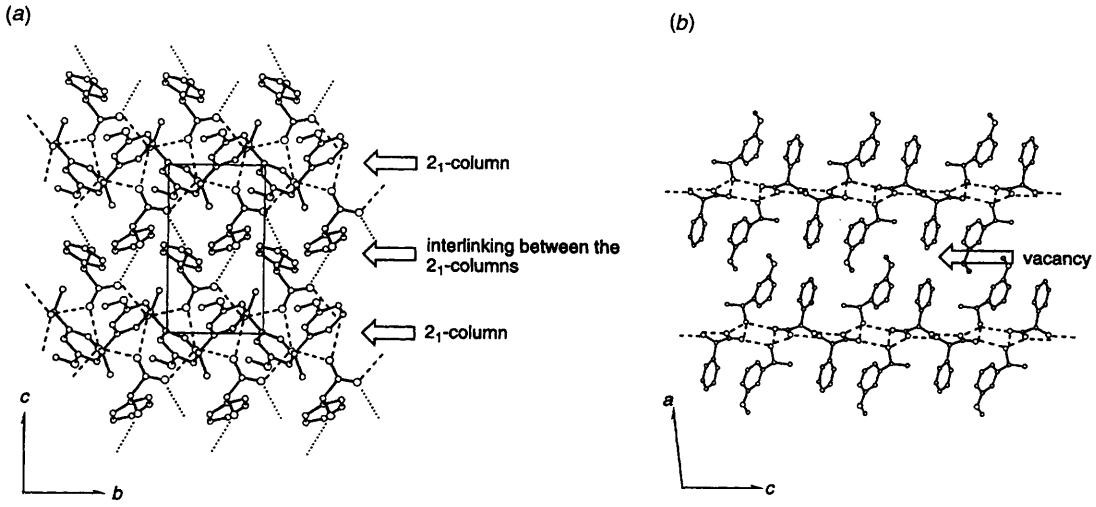

Fig. 6 Crystal structure of more-soluble (*S*)-**1**·(*R*)-**5**. (*a*) Viewed down the *a* axis. The dashed lines indicate the hydrogen bonds, which form the columns. The dotted lines indicate the hydrogen bonds, which interlink the columns. The solid lines show the unit cell. (*b*) Viewed down the *b* axis. The dashed lines show the hydrogen bonds.

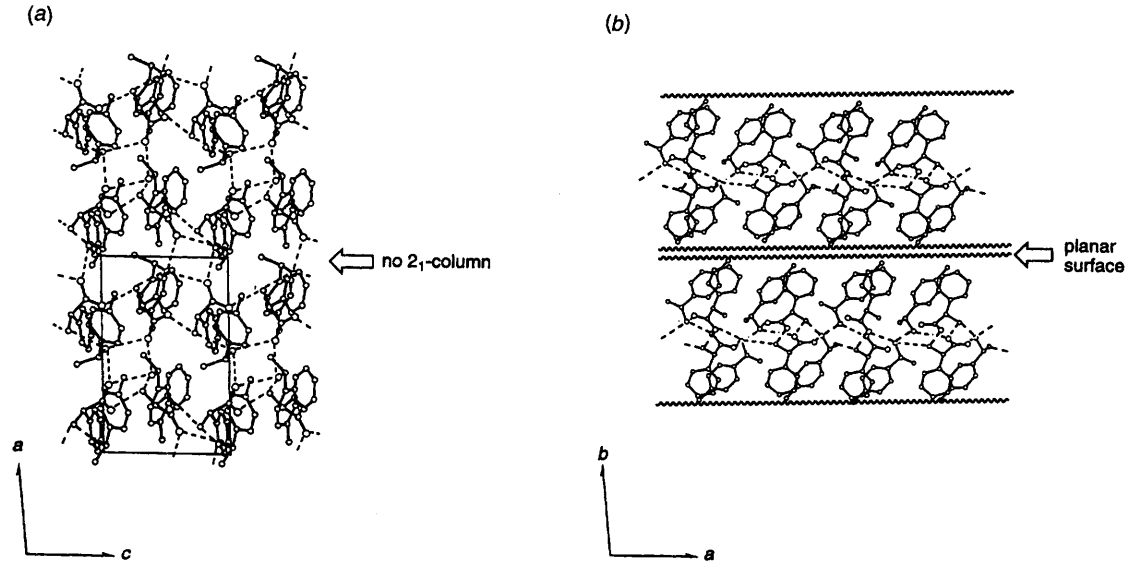

Fig. 7 Crystal structure of (*R*)-**1**·(*R*)-**8**. (*a*) Viewed down the *b* axis. The solid and dashed lines show the unit cell and hydrogen bonds, respectively. (*b*) Viewed down the *c* axis. The dashed lines show the hydrogen bonds. The wavy lines show the boundary surfaces of the layer.

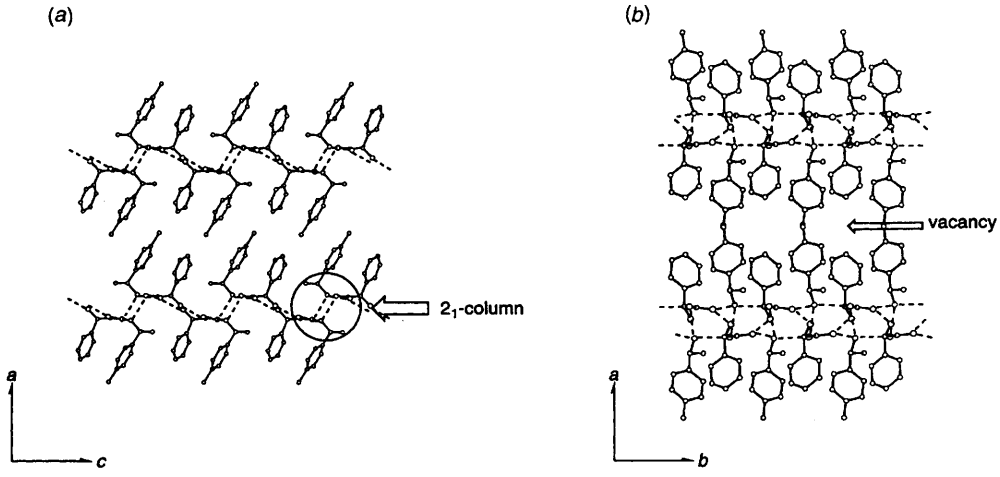

Fig. 8 Crystal structure of (*R*)-**1**·(*S*)-**8**: (*a*) Viewed down the *b* axis. The dashed lines indicate the hydrogen bonds. (*b*) Viewed down the *c* axis. The dashed lines show the hydrogen bonds.

similar to that of more-soluble (*S*)-**1**·(*R*)-**5** (Fig. 8); there is a hydrogen-bond layer formed by interlinked 2_1-columns, suggesting that this structure is stable from the viewpoint of its hydrogen-bonding interactions. However, the methyl group on the phenyl group of **8** projects out of the layer, and makes the boundary surfaces of the latter uneven [Fig. 8(*b*)]. This deformation apparently results in a looser packing of the layers; packing of the layers is insufficiently stabilised by van der Waals interactions between them.

Thus, in both (*R*)-**1**·(*R*)-**8** and (*R*)-**1**·(*S*)-**8**, stable hydrogen-bond layers, comprising 2_1-columns and having planar boundary surfaces, are not realised; these crystals are stabilised only by either hydrogen-bonding or van der Waals interactions. The difference in stability of the crystals of a pair of the diastereomeric salts affects their difference in solubility to a large extent. Therefore, the difference in solubility between (*R*)-**1**·(*R*)-**8** and (*R*)-**1**·(*S*)-**8** is diminished, resulting in the simultaneous deposition of both of the diastereomeric salts, namely, failure of the optical resolution.

Unfortunately, the crystal structures of the other diastereomeric salts of 1-arylethylamines with **1** could not be determined. However, the results of the crystallographic analysis that were performed, showing that there is a high correlation between the efficiency of the resolution of a target racemic 1-arylethylamine with a resolving reagent and the similarity in their molecular length, can be interpreted as follows. When the molecular length of a racemic 1-arylethylamine is similar to that of a resolving reagent, an infinite layer, consisting of 2_1-columns and having planar boundary surfaces, is realised in one of the two diastereomeric salts, which is favourable from the viewpoint of both hydrogen-bonding and van der Waals interactions (Fig. 9, type A). In contrast, when a substituent, increasing the molecular length, is introduced into the phenyl group of a 1-arylethylamine, the substituent tends to project out of the boundary surfaces of the hydrogen-bond layer consisting of 2_1-columns (type B). As a consequence the packing of the layers becomes loose; otherwise, if such loose packing of the layers is energetically too unfavourable, another pattern of hydrogen bonds appears enabling closer packing of the layers (type C), although the pattern of the hydrogen bonds becomes less favourable.[10] Hence, the crystal is stabilised only by either hydrogen-bonding or van der Waals interactions.

The difference in stability of the crystals of a pair of the diastereomeric salts affects their difference in solubility to a large extent. Hence in order to achieve a large difference in solubility between a pair of diastereomeric salts, it is necessary to achieve a large difference in stability between them through

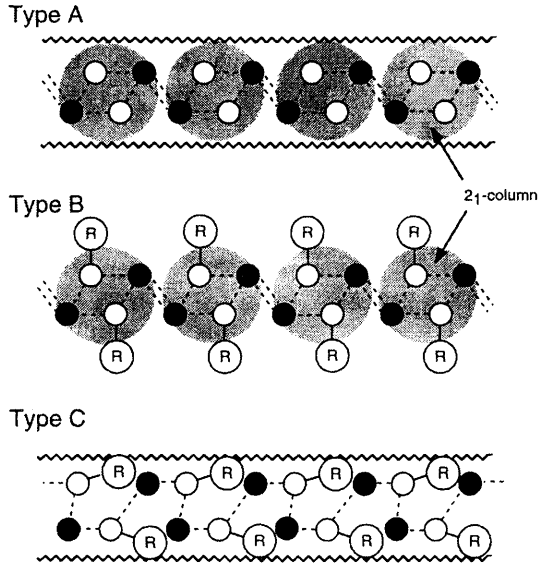

Fig. 9 Schematic representations of hydrogen-bond layers in the crystals of the diastereomeric salts of 1-arylethylamines with **1**. The black and white spheres represent **1** anion and 1-arylethylammonium cation, respectively. The dashed lines represent hydrogen bonds. Type A: crystal structures of less-soluble (*R*)-**1**·(*R*)-**3**, (*R*)-**1**·(*S*)-**4** and (*R*)-**1**·(*R*)-**5**. The wavy lines show the boundary surfaces of the layer. Type B: crystal structures of more-soluble (*S*)-**1**·(*R*)-**5** and unresolved (*R*)-**1**·(*S*)-**8**. R represents the substituent on the phenyl group of **5** or **8**. Type C: crystal structures of more-soluble (*S*)-**1**·(*R*)-**3** and unresolved (*R*)-**1**·(*R*)-**8**. The wavy lines show the boundary surfaces of the layer.

the formation of a stable hydrogen-bond network of type A in the crystal of one. The failure to resolve *p*- and some *m*-substituted 1-arylethylamines with (*R*)-**1** can be ascribed to the projection of the substituent on the aromatic group of the amines out of the boundary surfaces preventing the formation of a hydrogen-bond layer of type A, and causing a less-stable hydrogen-bond network of type B or C to be assumed.

Crystal structure of less-soluble (*R*)-**2**·(*R*)-**3** and (*R*)-**2**·(*R*)-**8**

We next went on to study the crystal structures of the less-soluble salts of **3** and **8** with (*R*)-**2**. Our previous results[3] showed that (*R*)-**2** could efficiently resolve **8**, which could not be resolved by (*R*)-**1** (Table 1, entry 10). The crystal structure of less-soluble (*R*)-**2**·(*R*)-**8** reveals that a hydrogen-bond network similar to those of less-soluble (*R*)-**1**·(*R*)-**3**, (*R*)-**1**·(*S*)-**4** and (*R*)-**1**·(*R*)-**5** is also formed in this crystal [Fig. 10(*a*)]; 2_1-columns are formed between the carboxylate and ammonium

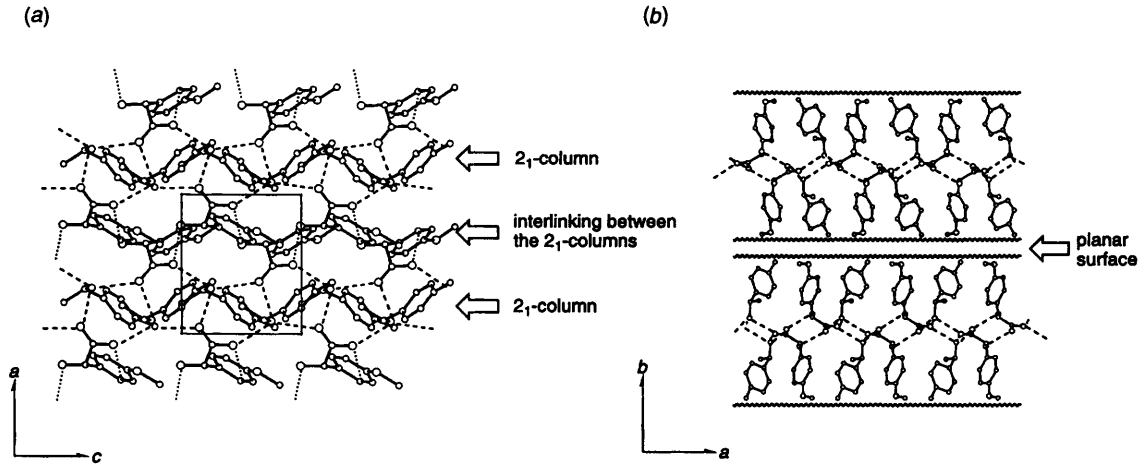

Fig. 10 Crystal structure of less-soluble (*R*)-**2**·(*R*)-**8**. (*a*) Viewed down the *b* axis. The dashed lines indicate the hydrogen bonds, which form the columns. The dotted lines indicate the hydrogen bonds, which interlink the columns. The solid lines show the unit cell. (*b*) Viewed down the *c* axis. The dashed lines show the hydrogen bonds. The wavy lines show the boundary surfaces of the layer.

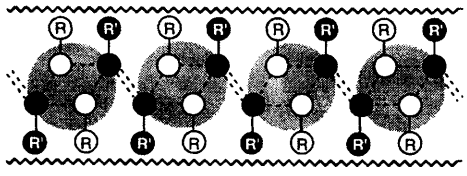

Fig. 11 Schematic image of the effect of the *p*-substituent of the phenyl group of **2**. The black and white spheres represent **2** anion and **8** cation, respectively. R and R′ represent the *p*-substituents of the phenyl groups of **8** and **2**, respectively.

groups, and a layered network is constructed by linkage of the 2_1-columns. As mentioned above, we ascribe the failure of the resolution of **8** with (*R*)-**1** to the projection of the *p*-substituent of the amine out of the hydrogen-bond layer consisting of 2_1-columns. In contrast, in the crystal structure of (*R*)-**2**·(*R*)-**8**, both the methoxy group of (*R*)-**2** and the *p*-methyl group of **8** project out of the layer making its boundary surfaces planar. As a result, a crystal structure stable from the viewpoint of both its hydrogen-bonding and van der Waals interactions is realised, as represented schematically in Fig. 11.

These results rationalise our previous proposal that the complementarity in size between a racemate and a resolving reagent is a fundamental and important factor in successful resolution;[3] when a racemate and a resolving reagent have similar molecular lengths, one of the enantiomers of the racemate can form a hydrogen-bond layer, consisting of 2_1-columns and having planar boundary surfaces, with the resolving reagent. Such a crystal preferentially precipitates upon crystallisation.

A similar hydrogen-bond layer was also found in the crystals of less-soluble (*R*)-**2**·(*R*)-**3**, which was also preferentially precipitated upon crystallisation (Table 1, entry 7). It is noteworthy that, as well as 2_1-columns being formed, the planarity of the boundary surfaces of the layer is preserved despite the presence of a *p*-substituent on (*R*)-**2** (Fig. 12). This crystal structure indicates that (*R*)-**2** recognises 1-arylethylamines by almost the same hydrogen-bond framework; the amine molecule fits in the framework, which is formed by (*R*)-**2** and is flexible to some extent, to realise a hydrogen-bond layer, consisting of columnar hydrogen bonds and having planar boundary surfaces. This means that when the molecular length of a racemic amine is somewhat shorter than that of the resolving acid being used, the carboxylate molecules can change their conformation to some extent to make the boundary surfaces of the layer planar, maintaining the interlinking of 2_1-columns.

Conclusions

The comparison of the crystal structures of the diastereomeric salts of 1-arylethylamines with (*R*)-**1** or (*R*)-**2** showed that the formation of a hydrogen-bond layer, consisting of 2_1-columns and having planar boundary surfaces, in one of a pair of the diastereomeric salts is necessary for efficient resolution. In order to realise such a hydrogen-bond layer, the molecular length of the racemate should be similar to or a little shorter than that of the resolving reagent being used.

Experimental

General

The IR spectra were recorded on a JASCO IR-810 spectrophotometer, and the ^{1}H NMR spectra were measured on a JEOL PMX-60SI or a JEOL GX-400 instrument using $SiMe_4$ as an internal standard. (*R*)-**1** and amines **3** and **8** were purchased from Yamakawa Chemical Industries, Inc.

Preparation of 1-arylethylamines

Racemic amines **4**–**7** were prepared by reductive amination of the corresponding ketones. To a solution of a ketone (40 mmol) in methanol (100 cm^3) was added ammonium acetate (0.5 mol) in one portion at room temperature. After the mixture had been stirred for 15 min, sodium cyanoborohydride (40 mmol) was added to it in one portion at room temperature. After being stirred for 2 d, hydrochloric acid (1 mol dm^{-3}; 150 cm^3) was added to the reaction mixture. The resulting mixture was washed with diethyl ether (2 × 50 cm^3), and then the aqueous phase was basified to pH = 10 with sodium hydroxide (*ca.* 0.6 mol). The liberated amine was extracted with dichloromethane (3 × 50 cm^3), and the combined extracts were dried (anhydrous potassium carbonate). After removal of the solvent under reduced pressure, the crude amine, obtained as a colourless oil, was purified by distillation *in vacuo*.

Preparation of racemic *p*-methoxymandelic acid (2)

The racemic acid was prepared from the corresponding aldehyde by the phase-transfer method reported by Merz.[11] To a solution of *p*-methoxybenzaldehyde (27.23 g, 0.20 mol) and benzyltriethylammonium chloride (2.48 g, 10 mmol) in chloroform (30 cm^3) was added aqueous sodium hydroxide (50%; 50 cm^3) at 56 ± 2 °C at a rate of one or two drops per min. After standing the mixture overnight at room temperature, the reaction mixture was poured into water (50 cm^3). The resulting mixture was washed with diethyl ether (2 × 30 cm^3), and the aqueous phase was separated and acidified with concentrated sul-

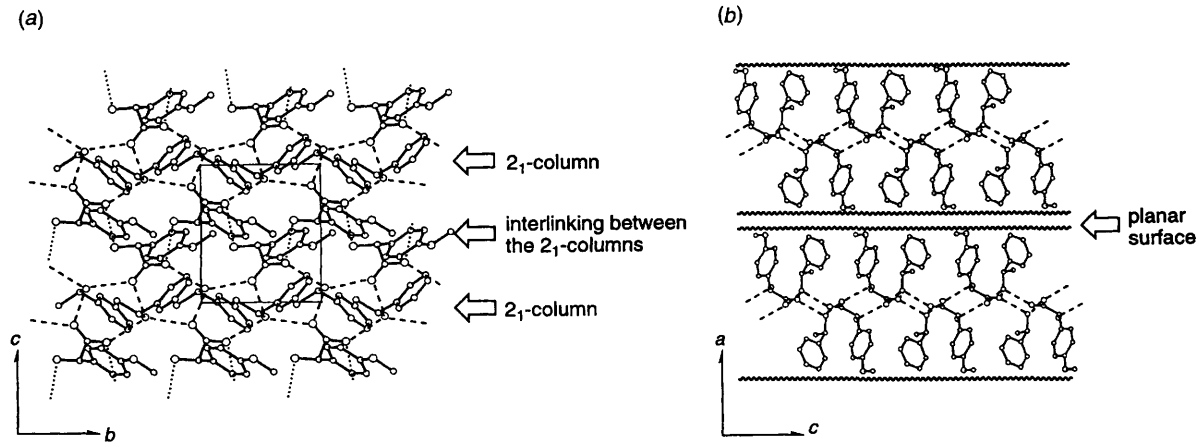

Fig. 12 Crystal structure of less-soluble (*R*)-**2**·(*R*)-**3**. (*a*) Viewed down the *a* axis. The dashed lines indicate the hydrogen bonds, which form the columns. The dotted lines indicate the hydrogen bonds, which interlink the columns. The solid lines show the unit cell. (*b*) Viewed down the *b* axis. The dashed lines show the hydrogen bonds. The wavy lines show the boundary surfaces of the layer.

Table 2 Summary of the crystal data of the diastereomeric salts

Compound	(*R*)-**1**·(*S*)-**4** (less soluble)	(*S*)-**1**·(*R*)-**5** (more soluble)	(*R*)-**1**·(*S*)-**8**	(*R*)-**1**·(*R*)-**8**	(*R*)-**2**·(*R*)-**3** (less soluble)	(*R*)-**2**·(*R*)-**8**[b] (less soluble)
Crystal system	Monoclinic	Monoclinic	Monoclinic	Triclinic	Monoclinic	Monoclinic
Space group	$P2_1$	$P2_1$	$C2$	$P\bar{1}$	$P2_1$	$P2_1$
a/Å	13.660(4)	13.110(2)	29.368(3)	13.331(2)	13.963(3)	8.269(4)
b/Å	5.714(2)	5.808(2)	6.0180(8)	14.410(3)	6.945(2)	29.849(9)
c/Å	10.365(2)	10.452(2)	9.0952(9)	8.300(2)	8.355(2)	6.885(3)
α(°)				98.05(2)		
β(°)	101.40(2)	95.85(2)	90.570(9)	90.50(1)	96.19(2)	90.25(4)
γ(°)				98.46(1)		
V/Å^3	793.1(4)	791.6(3)	1607.4(3)	1560.8(5)	805.5(4)	1700(1)
Z	2	2	4	4	2	4
D_c/g cm^{-3}	1.20	1.20	1.19	1.22	1.20	1.16
Crystal size	1.0 × 0.1 × 0.05	0.9 × 0.3 × 0.15	1.5 × 0.15 × 0.15	0.8 × 0.2 × 0.1	0.7 × 0.3 × 0.1	0.5 × 0.5 × 0.1
No. of parameters	210	282	255	766	282	430
Used reflections	984	1379	1386	4491	1370	2691
R[a]	0.055	0.045	0.063	0.059	0.033	0.130
R_w	0.062	0.048	0.070	0.061	0.035	0.149

[a] $R = \Sigma(||F_o| - |F_c||)/\Sigma(|F_o|)$. [b] We could not prepare a single crystal having sufficient quality for the X-ray analysis.

furic acid. The resultant oil was extracted with diethyl ether (2 × 50 cm^3), and the combined extracts were dried (anhydrous magnesium sulfate). Upon removal of the solvent under reduced pressure, the crude acid was obtained as a viscous oil (17.55 g, 48% yield). The crude acid was used without further purification for the following optical resolution.

Optical resolution of 2[12]

To a solution of **2** (13.6 g, 75 mmol) in methanol (20 cm^3) was added (*R*)-1-phenylethylamine (9.6 g, 78 mmol). After the mixture had been stirred for 2 h at room temperature, the precipitated crystalline salt was collected by filtration. The salt was recrystallised twice from methanol (80 then 60 cm^3) to afford a white crystalline salt (3.62 g, 32% yield, mp 188–196 °C). This salt was dissolved in water (50 cm^3), and the resulting solution was acidified with hydrochloric acid (1 mol dm^{-3}; 50 cm^3). The oil that appeared was extracted with diethyl ether (3 × 50 cm^3), and the combined extracts were dried (anhydrous magnesium sulfate). Upon removal of the solvent under reduced pressure, the crude acid was obtained as a white solid. The crude acid was purified by recrystallisation from benzene (30 cm^3) to afford chemically pure (*R*)-**2** (1.96 g, 26% yield). (*R*)-**2**: mp *ca.* 103–104 °C; $[\alpha]_D^{18}$ −143.6 (*c* 0.3, H_2O) [lit.,[12] mp *ca.* 104–105 °C; $[\alpha]_D^{25}$ −145.2 (*c* 0.3, H_2O)].

Treatment of an aliquot of (*R*)-**2** with diazomethane afforded the corresponding methyl ester quantitatively. The HPLC analysis (Daicel Chiralcel OJ) of the ester indicated that the enantiomeric excess of (*R*)-**2** was 95%.

Crystal structure determination and refinement

Crystals for X-ray analyses were prepared by slow evaporation of the solvent from a saturated solution in water for (*R*)-**1**·(*S*)-**4**, (*R*)-**1**·(*S*)-**8**, (*R*)-**1**·(*R*)-**8**, (*R*)-**2**·(*R*)-**3** and (*R*)-**2**·(*R*)-**8**. In the case of (*S*)-**1**·(*R*)-**5**, a single crystal was prepared by standing an ethanol solution of the salt in a sample tube saturated with diethyl ether vapour.

The X-ray intensities were measured up to $2\theta = 130°$ with graphite-monochromated Cu-Kα radiation (λ = 1.5418 Å) on a Mac Science MXC18 four-circle diffractometer by a 2θ–ω scan. All of the data were collected at room temperature. The cell dimensions were determined from about 20 reflections ($50° < 2\theta < 60°$). The intensities and orientation of the crystals were checked by three standard reflections every 100 reflections.

The structures were solved and refined by applying the CRYSTAN-GM package.[13] All of the non-hydrogen atoms were refined anisotropically. Hydrogen atoms were localised from a difference Fourier synthesis, except for (*R*)-**1**·(*S*)-**4**, (*R*)-**1**·(*R*)-**8** and (*R*)-**2**·(*R*)-**8**. The isotropic thermal parameters of the hydrogen atoms were fixed in the cases of (*R*)-**1**·(*S*)-**4**, (*R*)-**1**·(*R*)-**8** and (*R*)-**2**·(*R*)-**8**, and refined in all other cases. The lattice parameters and the final *R* factors for (*R*)-**1**·(*S*)-**4**, (*S*)-**1**·(*R*)-**5**, (*R*)-**1**·(*S*)-**8**, (*R*)-**1**·(*R*)-**8**, (*R*)-**2**·(*R*)-**3** and (*R*)-**2**·(*R*)-**8** are summarised in Table 2.

Atomic coordinates, bond lengths and angles, and thermal parameters for all diastereomeric salts have been deposited at the Cambridge Crystallographic Data Centre (CCDC). For details of the deposition scheme, see 'Instructions for Authors',

J. Chem. Soc., Perkin Trans. 2, 1996, Issue 1. Any request to the CCDC for this material should quote the full literature citation and the reference number 188/35.

Acknowledgements

The present work was supported by Grants-in-Aid for Scientific Research (Nos. 07555581, 06242101 and 06004310) from the Ministry of Education, Science, Sports and Culture of Japan. K. K. is grateful for a Research Fellowship of the Japan Society for the Promotion of Science for Young Scientists.

References

1 J. Jacques, A. Collet and S. H. Wilen, *Enantiomers, Racemates, and Resolutions*, Krieger Publishing Company, Malabar, Florida, 1994.
2 P. M.-C. Brianso, *Acta Crystallogr., Sect. B*, 1976, **32**, 3040; R. O. Gould and M. D. Walkinshaw, *J. Am. Chem. Soc.*, 1984, **106**, 7840; R. O. Gould, R. Kelly and M. D. Walkinshaw, *J. Chem. Soc., Perkin Trans. 2*, 1985, 847; A. Gorman, R. O. Gould, A. M. Gray, P. Taylor and M. D. Walkinshaw, *J. Chem. Soc., Perkin Trans. 2*, 1986, 739; E. Fogassy, M. Acs, F. Faigl, K. Simon, J. Rohonczy and Z. Ecsery, *J. Chem. Soc., Perkin Trans. 2*, 1986, 1881; R. O. Gould, P. Taylor and M. D. Walkinshaw, *Acta Crystallogr., Sect. C*, 1987, **43**, 2405; E. Fogassy, F. Faigl, M. Acs, K. Simon, E. Kozsda, B. Podanyi, M. Czugler and G. Reck, *J. Chem. Soc., Perkin Trans. 2*, 1988, 1385; M. Czugler, I. Csöregh, A. Kalman, F. Faigl and M. Acs, *J. Mol. Struct.*, 1989, **196**, 157; K. Simon, E. Kozsda, Z. Böcskei, F. Faigl, E. Fogassy and G. Reck, *J. Chem. Soc., Perkin Trans. 2*, 1990, 1395; M. Acs, E. Nwotny-Bregger, K. Simon and G. Argay, *J. Chem. Soc., Perkin Trans. 2*, 1992, 2011; K. Hatano, T. Takeda and R. Saito, *J. Chem. Soc., Perkin Trans. 2*, 1994, 579; R. Yoshida, O. Ohtsuki, T. Da-te, K. Okamura and M. Senuma, *Bull. Chem. Soc. Jpn.*, 1994, **67**, 3012.
3 K. Kinbara, K. Sakai, Y. Hashimoto, H. Nohira and K. Saigo, *Tetrahedron: Asymmetry*, 1996, **7**, 1539.
4 P. M.-C. Brianso, M. Leclercq and J. Jacques, *Acta Crystallogr., Sect. B*, 1979, **35**, 2751.
5 K. Sakai, Y. Hashimoto, K. Kinbara, K. Saigo, H. Murakami and H. Nohira, *Bull. Chem. Soc. Jpn.*, 1993, **66**, 3414.
6 The motif of this hydrogen-bond column can be described by graph sets as $C_2^1(4)C_2^2(6)[R_4^3(10)]$, see: M. C. Etter and J. C. MacDonald, *Acta Crystallogr., Sect. B*, 1990, **46**, 256.
7 K. Saigo, H. Kimoto, H. Nohira, K. Yanagi and M. Hasegawa, *Bull. Chem. Soc. Jpn.*, 1987, **60**, 3655; K. Kinbara, A. Kai, Y. Maekawa, Y. Hashimoto, S. Naruse, M. Hasegawa and K. Saigo, *J. Chem. Soc., Perkin Trans. 2*, 1996, 247; K. Kinbara, Y. Hashimoto, M. Sukegawa, H. Nohira and K. Saigo, *J. Am. Chem. Soc.*, 1996, **118**, 3441.
8 There are two reports on the crystal structure of (*S*)-**1**·(*R*)-**3** [(*R*)-**1**·(*S*)-**3**], see: K. Hashimoto, Y. Sumida, S. Terada and K. Okamura, *J. Mass Spectrom. Soc. Jpn.*, 1993, **41**, 87; H. L. de Diego, *Acta Chem. Scand.*, 1994, **48**, 306.
9 M. C. Etter, *Acc. Chem. Res.*, 1990, **23**, 120.
10 The effects of a substituent on a hydrogen-bond pattern have been reported. For example, see: J. A. Zerkowski, J. C. MacDonald, C. T. Seto, D. A. Wierda and G. M. Whitesides, *J. Am. Chem. Soc.*, 1994, **116**, 2382; J. A. Zerkowski and G. M. Whitesides, *J. Am. Chem. Soc.*, 1994, **116**, 4298.
11 A. Merz, *Synthesis*, 1974, 724.
12 J. R. E. Hoover, G. L. Dunn, D. R. Jakas, L. L. Lam, J. J. Taggart, J. R. Guarini and L. Phillips, *J. Med. Chem.*, 1974, **17**, 34.
13 CRYSTAN-GM, a computer program for the solution and refinement of crystal structures for X-ray diffraction data (MAC Science Corporation).

Paper 6/04179E
Received 13*th June* 1996
Accepted 19*th August* 1996